



CHORUS

This is the accepted manuscript made available via CHORUS. The article has been published as:

Plasmonic Brewster Angle: Broadband Extraordinary Transmission through Optical Gratings

Andrea Alù, Giuseppe D'Aguanno, Nadia Mattiucci, and Mark J. Bloemer

Phys. Rev. Lett. **106**, 123902 — Published 23 March 2011

DOI: [10.1103/PhysRevLett.106.123902](https://doi.org/10.1103/PhysRevLett.106.123902)

Plasmonic Brewster Angle: Broadband Extraordinary Transmission through Optical Gratings

Andrea Alù^{1,*}, Giuseppe D'Aguanno^{2,3}, Nadia Mattiucci^{2,3}, Mark J. Bloemer³

¹Dept. of ECE, University of Texas at Austin, Austin, TX 78712, USA

²AEgis Tech., Nanogenesis Division, Huntsville, AL 35806, USA

³Dept. of the Army, Charles M. Bowden Facility, Redstone Arsenal, AL 35898, USA

[*alu@mail.utexas.edu](mailto:alu@mail.utexas.edu)

Extraordinary optical transmission through metallic gratings is a well established effect based on the collective resonance of corrugated screens. Being based on plasmonic resonances, its bandwidth is inherently narrow, in particular for thick screens and narrow apertures. We introduce here a different mechanism to achieve total transmission through an otherwise opaque screen, based on an ultra-broadband tunneling that can span from DC to the visible range at a given incidence angle. This phenomenon effectively represents the equivalent of Brewster transmission for plasmonic and opaque screens.

PACS: 71.45.Gm, 41.20.Jb, 42.25.Ja, 42.79.Dj

The phenomenon of extraordinary optical transmission (EOT) through thin slits or apertures in a thick metal screen has been widely analyzed in the last decade [1]. The ratio of optical energy tunneling through an otherwise opaque screen versus the energy effectively impinging on the apertures may be made dramatically larger than unity, in particular for smaller apertures and larger periods. This anomalous transmission is based on multiple factors, including the excitation

of plasmonic and Fabry-Perot (FP) resonances, and other resonant effects supported by the periodicity of the corrugations [1]. A new class of optical devices based on EOT has been envisioned, such as light-emitting diodes, selective polarization filters and energy concentrators. One of the drawbacks of EOT for several of these applications is associated with the inherently narrow bandwidth of operation, which is directly associated with the resonant mechanisms on which it is based, in particular with the excitation of plasmonic and FP resonances. This becomes particularly relevant for smaller apertures and thicker screens, which are usually associated with larger Q-factor resonances. On the contrary, as long as the array period is rather small (below the first Bragg resonance), the EOT response is rather independent on the incidence angle. Here we introduce a dual EOT mechanism, inherently non-resonant, which may provide analogous levels of transmission enhancement over *ultrabroad* bandwidths, but for specific incidence angles. We show that this phenomenon is the analogous of Brewster transmission for corrugated plasmonic screens, providing minimized reflection for transverse-magnetic (TM) polarization, weakly dependent on frequency and on the screen thickness, but selective to the incidence angle. Independent of our findings, a recent letter has reported broadband transmission through narrow slits in the IR regime, based on spoof-surface plasmons [2]. Our results in the following extend these findings, showing that ultra-broadband transmission may be achieved without necessarily relying on plasmon resonances, but rather exploiting a non-resonant Brewster-like effect based on impedance matching.

Consider the geometry of Fig. 1: a metallic screen of thickness l , corrugated by slits of width w and period d , is illuminated by a TM wave. The scattering from such periodic structure is modeled here using a transmission-line (TL) approach, analogous to [3]. Due to the array periodicity, we can model the diffraction problem as its circuit analog depicted in the bottom of

Fig. 1, in which the free-space regions are modeled as semi-infinite TL and the slit region is treated as a TL segment of length l . For a given angle of incidence θ with respect to the z axis, the effective vacuum wave number is $\beta_0 = k_0 \cos \theta$, i.e., the longitudinal component of the impinging wave vector, and the characteristic impedance per unit length is $Z_0 = \eta_0 d \cos \theta$, calculated as the ratio between the voltage across one period $V_0 = \int_0^d E_x dx = |\mathbf{E}| d \cos \theta$ and the current per unit length $I_0 = H_y = |\mathbf{E}| / \eta_0$, and $\eta_0 = \sqrt{\mu_0 / \epsilon_0}$ is the vacuum impedance. Inside each slit, modal propagation does not depend on the incidence angle. The wave number β_s and characteristic impedance per unit length Z_s satisfy the equations [4]:

$$\begin{aligned} \tanh \left[\sqrt{\beta_s^2 - k_0^2} w / 2 \right] \sqrt{\beta_s^2 - k_0^2} &= -\sqrt{\beta_s^2 - k_0^2} \epsilon_m / \epsilon_m, \\ Z_s &= w \beta_s / (\omega \epsilon_0) \end{aligned} \quad (1)$$

where ϵ_m is the relative permittivity of the metal and Z_s is the ratio between $V_s = \int_0^w E_x dx = E_x w$ and $I_s = H_y = \omega \epsilon_0 E_x / \beta_s$. In deriving Eq. (1), we have assumed that the field penetration in the metal is very small, but we fully take into account the finite conductivity of the plasmonic material, its frequency dispersion and possible absorption, reflected in the dispersion of β_s and Z_s . This TL model holds as long as only the dominant *TM* mode propagates inside the slit and only the zero diffraction order radiates in free-space, i.e., $w \ll d < \lambda_0 = 2\pi / k_0$. In such circumstances, with good approximation the boundary conditions at the grating entrance and exit require that the equivalent voltages and currents are continuous, as in the circuit model of Fig. 1. More refined TL models [3] may consider also the presence of parasitic reactive elements at the two interfaces, taking into account the energy stored in the evanescent diffraction orders and in

the guided modes excited at the grating discontinuity, as well as the possible excitation of TE modes and the coupling among the slits. As we show in the following, these second-order effects are not significant in modeling the mechanisms described here.

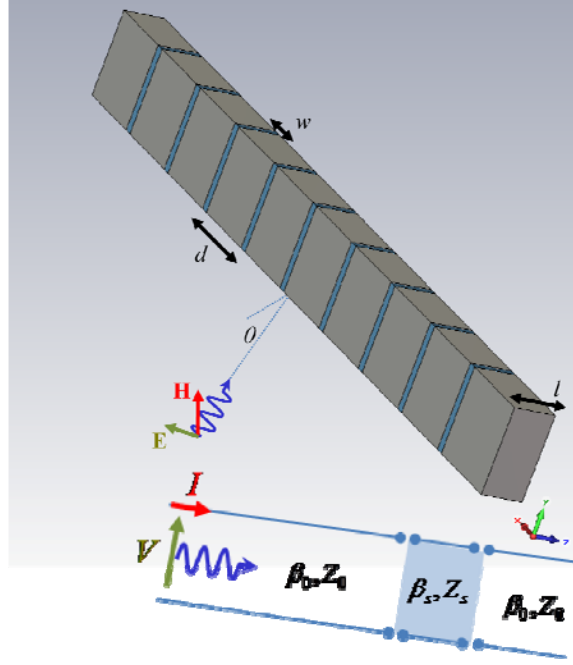


Figure 1 – Geometry of interest and its equivalent TL model.

In the limit of ultranarrow slits $w \ll d$, the effective slit impedance Z_s is inherently small compared to Z_0 for normal incidence, which physically corresponds to expectedly large reflections from such grating. The reflection coefficient at the grating entrance is generally written as:

$$R = \frac{[Z_s^2 - Z_0^2] \tan(\beta_s l)}{[Z_s^2 + Z_0^2] \tan(\beta_s l) + 2iZ_s Z_0}. \quad (2)$$

In the lossless limit, zero reflection and EOT is obtained at the usual FP resonances $\beta_s l = n\pi$, with n being an integer, consistent with the findings in [1]. EOT resonances are also achieved

when the grating period allows coupling to surface plasmons, or spoof surface plasmons for corrugated conducting screens [5]. This phenomenon is not captured by Eq. (2), since it involves higher-order propagating diffraction orders, which arise only for periods comparable or larger than λ_0 . Yet, Eq. (2) admits another peculiar condition for zero reflection, which arises when $Z_s = Z_0$, i.e., when the grating is anomalously *impedance matched* with free-space. For normal incidence this condition is hardly met, due to the opaqueness of metal but, by increasing the angle of incidence θ , Z_0 is smoothly reduced to zero as the tangential component of electric field is reduced. From Eq. (1), the anomalous matching condition is achieved at the angle θ_B :

$$\cos \theta_B = (\beta_s w) / (k_0 d), \quad (3)$$

which represents the effective *plasmonic Brewster angle*. This anomalous matching phenomenon is *totally independent* on the grating thickness, since the effective slit impedance matches the impinging wave at each interface, producing anomalous total tunneling and energy squeezing through each slit. This strikingly simple formula captures to a large degree a novel tunneling phenomenon, fully considering metal dispersion and absorption at higher frequencies. Different from FP and plasmon resonances [1]-[2], minimum reflection is achieved even when large absorption is present in the slits, of great interest for energy concentration and harvesting. In addition, condition (3) is weakly dependent on frequency, ensuring that this Brewster-like transmission provides ultra-broadband response, effectively extending from zero frequencies (DC) to the breakdown of this model $d \simeq \lambda_0$. For lower frequencies, the metal tends to become a perfect conductor, for which $\beta_s = k_0$ and $\theta_B = \cos^{-1}(w/d)$, close to the grazing angle for small

w/d . For higher frequencies, the plasmonic features of metal come into play, increasing β_s and correspondingly reducing θ_B .

It is important to stress that this effect is based on the modal propagation in ultranarrow slits, and it is therefore limited to 2-D apertures (slits). In some sense, this phenomenon is the dual of the energy squeezing and total transmission mechanism through ultranarrow channels filled with zero permittivity materials [6]. In [7], this effect was proven to be based on an analogous matching phenomenon, for which the inherently low impedance in an ultranarrow channel may be matched to a much thicker waveguide by using zero-permittivity fillings. Here, we can equivalently describe the wave interaction with the narrow slits as the one of an homogenized metamaterial slab with relative effective parameters $\epsilon_{eff}^{(s)} = d/w$, $\mu_{eff}^{(s)} = w(\beta_s^2/k_0^2 + \sin^2\theta)/d$, compared to the effective parameters in vacuum $\epsilon_{eff}^{(v)} = 1$, $\mu_{eff}^{(v)} = \cos^2\theta$. For small ratios w/d , $\epsilon_{eff}^{(s)}$ is very large while $\mu_{eff}^{(s)}$ is comparably low. However, at the plasmonic Brewster angle (3), the ratios $\mu_{eff}^{(v)}/\epsilon_{eff}^{(v)}$ and $\mu_{eff}^{(s)}/\epsilon_{eff}^{(s)}$ in the two effective materials coincide (i.e., $Z_0 = Z_s$), since the effective permeability of the impinging wave $\mu_{eff}^{(v)}$ tends effectively to zero, producing unitary transmission. Different from [6]-[7], here we do not need to fill the slits with zero permittivity metamaterials, as the outside medium naturally holds a very low effective permeability for large angles. This tunneling mechanism is the *exact physical analogous* of what happens in a dielectric slab with $\epsilon > \epsilon_0$ at the Brewster angle condition, for which the lower impedance of a dielectric etalon may be matched to free-space for TM incidence at an oblique angle. Brewster-like effects for metallic gratings have been discussed in the literature [8], but referring to quite different transmission mechanisms, mainly based on collective plasmonic resonances, largely frequency

dependent. Here, due to the absence of a resonance, this matching mechanism is inherently ultra-broadband, as we verify in the following with full-wave simulations.

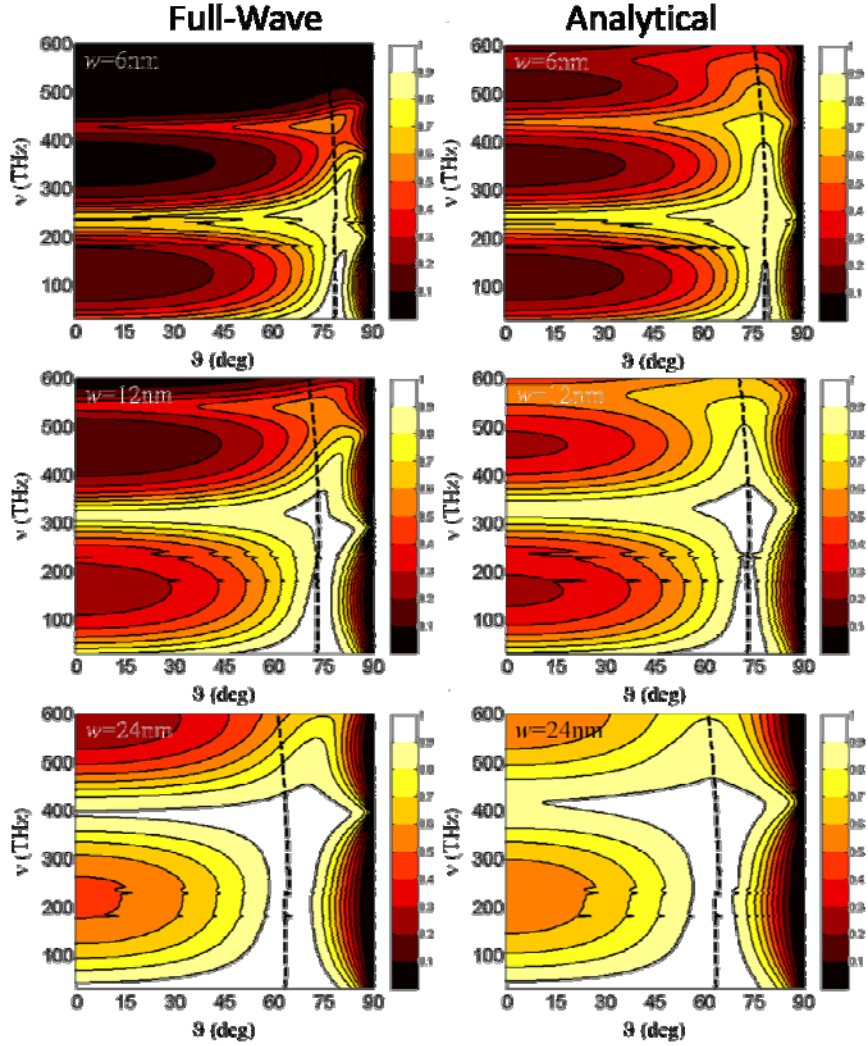


Figure 2 – Angular transmission spectra for a grating thickness $l = 200 \text{ nm}$ and period $d = 96 \text{ nm}$. The slit width is indicated in each panel. FMM simulations (left) are compared with analytical results (right). The dashed line indicates the plasmonic Brewster angle condition.

In Fig. 2, we show the calculated angular TM power transmission spectra for a grating with $l = 200 \text{ nm}$, $d = 96 \text{ nm}$, and various slits widths, as indicated in each panel. The left column

shows full-wave simulations based on the Fourier modal method (FMM) [9], compared in the right to our analytical model. We consider realistic experimental dispersion and loss of silver permittivity [10]. It is noticed how the TL model captures with extreme accuracy the fundamental physical mechanisms behind the transmission resonances of the grating. At normal incidence ($\theta = 0$), typical EOT peaks based on FP resonances are visible in all panels. For narrower slits (top row) such resonances are shifted to lower frequencies, due to their plasmonic features that ensure a larger $\text{Re}[\beta_s]$ for smaller w in (1). These resonances reflect in horizontal bands in the plots of Fig. 2, since this EOT mechanism is inherently narrow-band in frequency, but weakly dependent on the incidence angle.

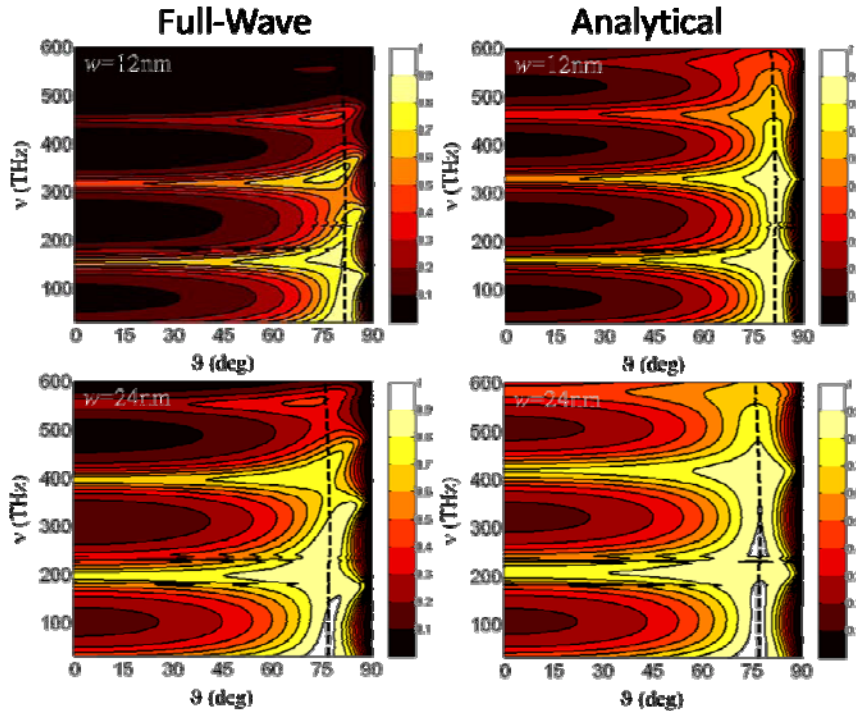


Figure 3 – Similar to Fig. 2, but for thicker screens and a larger period: $l = 400 \text{ nm}$ and

$$d = 192 \text{ nm} .$$

In contrast, the plasmonic Brewster transmission arises in all plots as a vertical band, confirming weak dependence on frequency, but strong selectivity to the transmission angle. Each plot reports, as a dashed line, the dispersion of the predicted Brewster angle (or better its real part, since losses are considered here), as in Eq. (3). For smaller ratios w/d , the plasmonic Brewster angle is closer to grazing, whereas for larger widths it moves towards smaller angles. The weak dispersion of the dashed line is due to the variation of $\text{Re}[\beta_s]$ with frequency, which somehow limits the bandwidth of this effect, and is followed with excellent precision by the transmission peak in the calculated full-wave spectra. For higher frequencies, the effect of absorption in the slit is evident, in particular for narrower widths, which reduces the transmission maxima and affects to some extent the precision of our analytical model. In any case, an ultra-broadband EOT phenomenon is verified by our full-wave simulations precisely at the angle θ_B . We have verified that, by further increasing the slit aperture for fixed period, the vertical transmission band shifts to smaller θ_B , judiciously following Eq. (3), even for very large slit apertures. Such extreme scenarios are of less interest, since the angular selectivity of the grating is compromised and energy squeezing is limited. In the supplemental material [11], we show a similar plot, but considering a larger grating period $d = 192 \text{ nm}$. The results are consistent with Fig. 2, and also here Brewster transmission is obtained over a broad frequency range from DC to the visible at the specific angle θ_B . In this second scenario, since the silver filling ratio is larger, angular selectivity and loss sensitivity are increased, due to larger energy squeezing.

Figure 3 shows analogous results, but for a thicker screen $l = 400 \text{ nm}$. As expected, the horizontal transmission bands typical of FP resonances have narrower bandwidths and are denser along the frequency spectrum, due to longer slits. However, the anomalous Brewster

transmission is weakly affected by the thickness, as confirmed by Eq. (3), since minimal reflection is expected at the entrance and exit faces of the screen, independent of the frequency of operation. Transmission is slightly reduced at higher frequencies in this example, due to the longer propagation through narrow slits.

This anomalous phenomenon would be available even if, at some section along the slit, we would add a matched absorbing material or an energy harvesting device, converting the tunneled energy into other forms. On the contrary, FP or plasmon resonances, based on multiple reflections or coupling between the slit entrance and exit [1]-[2], would be completely damped in such condition. This provides interesting venues to apply this matching phenomenon for energy concentration and harvesting.

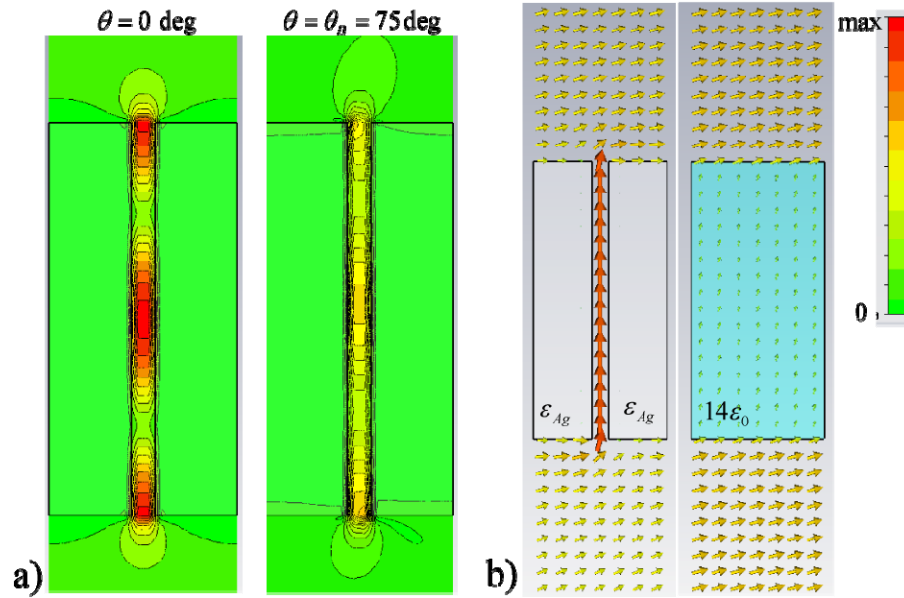


Figure 4 – (a) Electric field distribution E_x on the E plane for $l = 400 \text{ nm}$, $d = 192 \text{ nm}$, $w = 24 \text{ nm}$ at $f = 395 \text{ THz}$ for: normal incidence (left), incidence angle $\theta_B = 75 \text{ deg}$ (right). (b) Power flow distribution at the Brewster angle (left) and comparison with an equivalent dielectric etalon with $\epsilon = 14\epsilon_0$. In each panel the fields are normalized to the same scale.

In order to further highlight the anomalous features of this phenomenon, Fig. 4a shows the electric field amplitude (transverse to the slit) for the geometry of Fig. 3 (bottom row) at the frequency $f = 395 THz$, which represents the frequency of the second FP resonance of the grating ($\text{Re}[\beta_s]l = 2\pi$). In the left panel, we show the case of normal incidence excitation, whereas in the right panel we excite at the Brewster angle $\theta_B = 75 \text{ deg}$. It is evident how, despite both excitations ensure very high transmission, the field distributions inside the slit are very different. For normal incidence, total transmission is obtained by exploiting a strong FP resonance established via the large mismatch at entrance and exit face, which forms a typical standing wave distribution inside the slit. Obviously, this resonance is very sensitive to the geometry of the slit, the operating frequency and the presence of absorption along the slit. In contrast, at the Brewster condition, tunneling is based on impedance matching: the wave does not experience any change in effective impedance and it can tunnel through the slit with nearly uniform amplitude and minimum reflections. For sake of comparison, the scale in the two plots of Fig. 4a is the same, showing that the lack of resonance also reduces the peak field values in the slit and the associated stored energy, with obvious advantages in terms of robustness to loss and geometry variations. Consistent with Fig. 3, at this angle EOT is weakly dependent on frequency and possible presence of absorption or change in slit length. Even possible bending within the slit would not affect this matching behavior, allowing energy rerouting [6].

In Fig. 4b, we compare the power flow (Poynting vector) distribution at the Brewster condition with the one of an equivalent dielectric etalon with same length and $\epsilon = 14\epsilon_0$, which would support Brewster transmission at the same angle θ_B . Indeed, the slit openings in the plasmonic screen provide a tunneling mechanism that has analogous features to the usual Brewster

phenomenon, despite the opaqueness of the material forming the screen. Similar to a dielectric etalon, total transmission is obtained only for TM polarization. In fact, due to the choice of narrow slits, transverse-electric excitation would be totally reflected at all angles and all frequencies, ensuring strong polarization sensitivity, which may be used to realize ultrathin and ultra-broadband filter polarizers. To conclude, we have shown here that plasmonic gratings formed by ultranarrow slits and small periods may support ultra-broadband anomalous matching, analogous to Brewster transmission, despite the metal opaqueness. These results may be applied to novel polarization filters, energy concentrators and absorbers. Ultranarrow slits in plasmonic screens with aspect ratios similar to those considered in this letter may be obtained with advanced nanofabrication techniques, such as nanoskyving [12]. Moreover, by relaxing the requirements on the slit width and period, analogously broadband transmission mechanisms may be verified from DC to THz frequencies. In preparation for an experimental proof-of-concept of this anomalous phenomenon, we have also considered the presence of a glass substrate at the grating exit, verifying that its presence does not significantly influence the previous results.

References

- [1] T. W. Ebbesen, et al., *Nature* **391**, 667 (1998); F.J. García de Abajo, *Rev. Mod. Phys.* **79**, 1267 (2007); F. J. Garcia-Vidal, et al., *Rev. Mod. Phys.* **82**, 729 (2010).
- [2] X.R. Huang, R.W. Peng, R.H. Fan, *Phys. Rev. Lett.* **105**, 243901 (2010).
- [3] F. Medina, F. Mesa, R. Marques, *IEEE Trans. Microw. Th. Techn.* **56**, 3108 (2008); A. Fernandez-Prieto, F. Medina, F. Mesa, *Appl. Phys. Lett.* **95**, 021108 (2009).
- [4] A. Alù, N. Engheta, *J. Opt. Soc. Am. B* **23**, 571 (2006).
- [5] J. B. Pendry, L. Martin-Moreno, F. J. Garcia-Vidal, *Science* **305**, 847 (2004).

- [6] M. Silveirinha N. Engheta, *Phys. Rev. Lett.* **97**, 157403 (2006); B. Edwards, et al., *Phys. Rev. Lett.* **100**, 033903 (2008).
- [7] A. Alù, M. G. Silveirinha, N. Engheta, *Phys. Rev. E* **78**, 016604 (2008); A. Alù, N. Engheta, *Phys. Rev. Lett.* **103**, 043902 (2009).
- [8] L. B. Mashev, E. Popov, E. G. Loewen, *Appl. Opt.* **28**, 2538 (1989); E. Popov, S. Enoch, N. Bonod, *Opt. Expr.* **17**, 6770 (2009).
- [9] L. Li, *J. Opt. Soc. Am. A* **13**, 1870 (1996) and references therein.
- [10] E. D. Palik, *Handbook of Optical Constants of Solids*, Academic Press Inc., New York (1991).
- [11] EPAPS Fig. 1: Similar to Fig. 2, but for double period $d = 192 \text{ nm}$.
- [12] Q. Xu, R. M. Rioux, M. D. Dickey, G. M. Whitesides, *Acc. Chem. Res.* **41**, 1566 (2008).